Chapter 6

Stability analysis of steady-state solution

In this chapter an instability of the homogeneous solution of reaction-diffusion system leading to the formation of static stationary spatial patterns (Turing instability) is studied. In section 6.1 the general criteria of Turing instability for two-component system in general form and pattern selection problem are briefly discussed. As an example these criteria are considered in a frame work of a concrete two-component reaction-diffusion system (see section 6.2). The influence of the global feedback in form of an integral term on Turing instability conditions as well as on the resulting Turing patterns is presented in section 6.3. Finally, Turing instability in reaction-diffusion systems with more than two components is discussed in section 6.4.

6.1 Turing instability in general form

A Turing instability (or bifurcation) involves the destabilization of a homogeneus solution to form a static periodic spatial pattern (Turing pattern), whose wavelength depends on the local reaction kinetic parameters, diffusion coefficients of the system and is its intrinsic property. The hypothesis that just a difference in diffusion constants of components could be enough to destabilize the homogeneous solution was put forward by *A. M. Turing* in 1952 [Turing, 1952]. By studying the problem of biological morphogenesis he showed that a reaction-diffusion system with a different diffusion constants can autonomously produce stationary spatial patterns.

Over the years this idea have attached the attention of a great number of scientists. *I. Prigogine* and his coworkers have studied Turing patterns and other instabilities in details in so-called Brusselator model for hypothetical chemical reaction [Prigogine and Lefever, 1968, Prigogine, 1969]. *A. Gierer* and *H. Meinhardt* have proposed a model, called Gierer-Meinhardt thereafter [Gierer and Meinhardt, 1972], which is widely used to describe pattern

formation in living organisms. A systematic study of biological pattern formation has also been performed by *J. Murray* [Murray, 1993]. The first laboratory observation of Turing structures was made in 1990 by *P. De Kepper* and coworkers in Bordeaux in so-called CIMA reaction. Subsequent studies by *Q. Ouyang* and *H. L. Swinney* using the disk reactor showed quasi two-dimensional patterns in the form of hexagons and stripes [Ouyang and Swinney, 1991]. Other examples of Turing patterns and corresponding reaction-diffusion models can be found in, e.g., [Murray, 1993, Cross and Hohenberg, 1993, Maini et al., 1997].

6.1.1 Linear stability analysis

We start our analysis of Turing instability from by considering a reaction-diffusion system in general form, restricting ourself first to the case of two components, i.e.,

$$\partial_t \mathbf{u} = \mathbf{D}\nabla^2\mathbf{u} + \mathbf{R}(\mathbf{u}) \tag{6.1}$$

where $\mathbf{u} = \mathbf{u}(\mathbf{r}, \mathbf{t}) = (u, v)^T$ is a vector of concentration variables, $\mathbf{R}(\mathbf{u}) = (f(u, v), g(u, v))^T$ describes as before a local reaction kinetics and the Laplace operator ∇^2 acts on the vector $\mathbf{u}$ componentwise. $\mathbf{D}$ denotes a diagonal diffusion coefficient matrix,

$$\mathbf{D} = \begin{pmatrix} D_u & 0 \\ 0 & D_v \end{pmatrix}.$$

Note that we suppose the system 6.1 to be isotropic and homogeneous, so $\mathbf{D}$ is a scalar matrix, independent on coordinates.

Let $\mathbf{u_0} = (u_0, v_0)^T$ be a homogeneous solution (or steady-state solution) of the system (6.1), i.e. $f(u_0, v_0) = g(u_0, v_0) = 0$. Suppose that this solution is stable in absence of diffusion, namely the real parts of all eigenvalues of the Jacobi matrix

$$\mathbf{A} = (\partial\mathbf{R}/\partial\mathbf{u})_{\mathbf{u}=\mathbf{u_0}} = \begin{pmatrix} f_u & f_v \\ g_u & g_v \end{pmatrix}$$

describing the local dynamics of the system (6.1) are less that zero. For the case of a 2×2 matrix this is equivalent to the simple well-known condition for the trace and the determinant of the matrix $\mathbf{A}$, namely

$$\begin{aligned} \mathrm{Sp}(\mathbf{A}) &= f_u + g_v < 0 \\ \det(\mathbf{A}) &= f_u g_v - f_v g_u > 0. \end{aligned} \tag{6.2}$$

Keeping Eq. (6.2) in mind let us see if the presence of diffusion term can change the stability of $\mathbf{u_0}$. To this end, consider a small perturbation $\tilde{\mathbf{u}}$, i.e. $\mathbf{u} = \mathbf{u_0} + \tilde{\mathbf{u}}$ and the corresponding linear equation for it:

$$\partial_t \tilde{\mathbf{u}} = \mathbf{D}\nabla^2\tilde{\mathbf{u}} + \mathbf{A}\tilde{\mathbf{u}}. \tag{6.3}$$

After decomposition $\tilde{\mathbf{u}}$ into modes $\tilde{\mathbf{u}} \sim \mathbf{a_k} e^{ikr}$ we get the equation

$$\dot{\mathbf{a}}_\mathbf{k} = \mathbf{B}\mathbf{a}_\mathbf{k}, \tag{6.4}$$

where $\mathbf{B} = \mathbf{A} - k^2\mathbf{D}$.

As we have previously mentioned the stability conditions for the system (6.4) with a 2×2 matrix $\mathbf{B}$ can be written as:

$$\begin{aligned} \mathrm{Sp}(\mathbf{B}) < 0 \quad \forall k \\ \det(\mathbf{B}) > 0 \quad \forall k, \end{aligned} \tag{6.5}$$

where

$$\mathrm{Sp}(\mathbf{B}) = -(D_u + D_v)k^2 + \mathrm{Sp}(\mathbf{A}), \tag{6.6}$$

$$\det(\mathbf{B}) = D_u D_v k^4 - (D_u g_v + D_v f_u)k^2 + \det(\mathbf{A}). \tag{6.7}$$

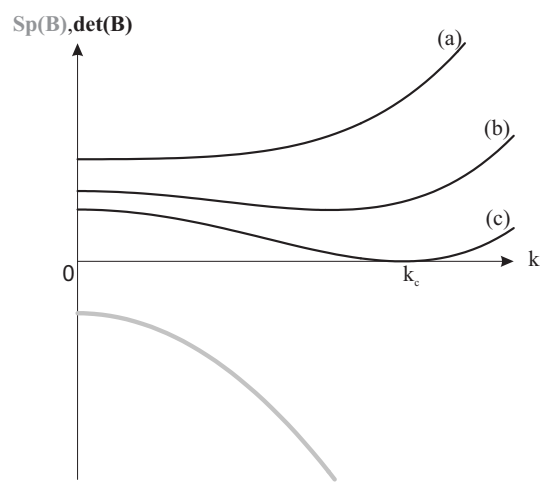

FIG. 6.1: Dependence $\mathrm{Sp}(\mathbf{B})$ and $\det(\mathbf{B})$ on wave vector k. The gray curve illustrate the fact that $\mathrm{Sp}(\mathbf{B}) < 0 \ \forall \ k$, whereas black lines show three typical behaviors of the function $T(k) = \det(\mathbf{B})$: (a) $T(k) > 0 \ \forall \ k$; (b) $T(k)$ is positive $\forall \ k$, but has a minimum for $k > 0$; (c) onset of instability: $T(k) = 0$ for $k = k_c$.

Notice, that for $k = 0$ the conditions (6.5) are equivalent to the stability criterion (6.2) for the local dynamics. In particular this implies that $\mathrm{Sp}(\mathbf{B}) < 0$ for all k (see gray curve in Fig. 6.1 for illustration), so the instability of the homogeneous solution can occur only due to violation of the second condition (6.5), that is, $\det(\mathbf{B})$ should be equal to zero for some k. It means that the instability occur at the point where the equation $\det(\mathbf{B}) = 0$ has a multiple root. To find it we can simply calculate a minimum of the function $T(k) = \det(\mathbf{B})$.

$$T'(k) = 4D_u D_v k^3 - 2(D_u g_v + D_v f_u)k = 0 \quad \Rightarrow \quad k^2 = \frac{1}{2}\left(\frac{f_u}{D_u} + \frac{g_v}{D_v}\right)$$

From the last equation can be seen that the described above situation is possible if

$$D_u g_v + D_v f_u > 0 \tag{6.8}$$

In this case the critical wavenumber is

$$k_c = \sqrt{\frac{1}{2}\left(\frac{f_u}{D_u} + \frac{g_v}{D_v}\right)} \tag{6.9}$$

and instability occurs on condition that

$$T(k_c) \leq 0 \quad \Leftrightarrow \quad k_c^4 = \left(\frac{1}{2}\left(\frac{f_u}{D_u} + \frac{g_v}{D_v}\right)\right)^2 > \frac{\det\mathbf{A}}{D_u D_v} \tag{6.10}$$

The instability scenario, described above is illustrated in Fig. 6.1, where three different cases of dependence of the function $T(k) = \det(\mathbf{B})$ on the wave vector k are presented. In Fig. 6.1(a) the function $T(k)$ has no roots, so the stability of $\mathbf{u_0}$ is not affected as well as in the case (b). Here $T(k) > 0$ for all k, but minimum of this function exists. Finally, in Fig. 6.1(c) $T(k) = 0$ for $k = k_c$, indicating the onset of instability.

Hence, the full system of the conditions for instability of the homogeneous solution $\mathbf{u_0}$ is

$$\begin{aligned} f_u + g_v &< 0, \\ f_u g_v - f_v g_u &> 0, \\ D_u g_v + D_v f_u &> 0, \\ \left(\frac{f_u}{D_u} + \frac{g_v}{D_v}\right)^2 &> \frac{4\det\mathbf{A}}{D_u D_v}. \end{aligned} \tag{6.11}$$

A detailed description of the mechanism of Turing instability can also be found in [Murray, 1993, Mikhailov, 1990, Kapral, 1995].

Remark: Apart from the Turing instability, *a Hopf instability* can be encountered if condition (6.2)(or the first condition (6.5)) is violated. In this case, after initial growth of the critical mode, the evolution of the system is determined by the nonlinear part of the reaction function and is a subject of nonlinear stability analysis, which was discussed in details in, e.g., [Kuramoto, 1984]. As result, the system either operates in supercritical regime, that is, admits spatially homogeneous periodic oscillations, or in subcritical one, whereby the system can be driven far away from the homogeneous solution $\mathbf{u_0}$.

6.1.2 Activator-inhibitor principe and pattern selection

Let us discuss the system of instability conditions obtained above. Consider the first and the third equations of (6.11). As is easy to see f_u and g_v should have different signs. Furthermore analysis of other conditions (6.11) shows that only four possible combinations of signs for components of the Jacobi matrix $\mathbf{A}$ do not affect (6.11):

$$\begin{pmatrix} + & - \\ + & - \end{pmatrix} \quad \begin{pmatrix} + & + \\ - & - \end{pmatrix} \quad \begin{pmatrix} - & + \\ - & + \end{pmatrix} \quad \begin{pmatrix} - & - \\ + & + \end{pmatrix}$$

If $f_u > 0$ and $g_v < 0$ we say species u is *the activator* and species v is *the inhibitor*. In what follows we are concentrated just on the systems from this class. Furthermore we have $\frac{D_u}{D_v} < 1$, i.e., the diffusion coefficient of the inhibitor should be greater that of the activator.

While the conditions for the onset of a Turing bifurcation are rather simple, the determination of the nature of the pattern that is selected is a more difficult problem since beyond the bifurcation point a finite band of wavenumbers is unstable. Pattern selection is usually approached by studying *amplitude equations* that are valid near the onset of the instability. To determine which modes are selected, modes and their complex conjugates are usually treated in pairs so that the concentration field, expanded about the homogeneous solution, reads

$$\mathbf{u}(\mathbf{r}, t) = \mathbf{u_0} + \sum_{j=1}^{n} \big(A_j(t) e^{i\mathbf{k_j r}} + c.c\big),$$

where $\mathbf{k_j}$ are different wavevectors such that $|\mathbf{k_j}| = k_c$. In one dimensional space the situation is rather simple, as result of the instability is represented by a periodic in space structure. In two space dimension this form leads to *stripes* for $n = 1$, *rhombi* (or *squares*) for $n = 2$ and *hexagons* for $n = 3$. The pattern and wavelength that is selected depends on coefficients in the nonlinear amplitude equation for the complex amplitude A_j, but some conclusions about selected pattern can be made using, e.g., symmetry arguments. In particular, in the case of hexagonal pattern, in which three wave vectors are mutually situated at an angle of $2\pi/3$, i.e., $\mathbf{k_1} + \mathbf{k_2} + \mathbf{k_3} = 0$, the absence of inversion symmetry ($\mathbf{u} \mapsto -\mathbf{u}$) leads to additional quadratic nonlinearity in the amplitude equation. The latter, in its turn, ends in a fact, that hexagonal pattern has the maximum growth rate near the threshold and is therefor preferred (for details see [Cross and Hohenberg, 1993]).

The general procedure in details for the derivation of such amplitude equations based on mode projection techniques can be found in [Haken, 1983]. Another approach, using multi scale expansion was evolved in [Newell and Whitehead, 1971].

6.2 Turing instability in two-component RD system

Now let us consider as an example of Turing instability a following two-component reaction-diffusion system of the form (**see...**)

$$\begin{aligned} \partial_t u &= D_u \Delta u + f(u) - v + \kappa_1, \\ \tau \partial_t v &= D_v \Delta v + u - v, \end{aligned} \tag{6.12}$$

where $f(u) = \lambda u - u^3$. Here $u = u(r,t)$ and $v = v(r,t)$ denote the activating and inhibiting components correspondingly. The parameters D_u, D_v, τ, λ are positive, whereas the sign of κ_1 is arbitrary.

The steady-state solutions (u_0, v_0) can be found solving

$$\begin{aligned} (\lambda - 1)u_0 - u_0^3 + \kappa_1 &= 0, \\ v_0 &= u_0. \end{aligned} \tag{6.13}$$

For the system (6.12) the matrices $\mathbf{D}, \mathbf{A}$ and $\mathbf{B}$ are given by

$$\mathbf{D} = \begin{pmatrix} D_u & 0 \\ 0 & D_v/\tau \end{pmatrix}, \quad \mathbf{A} = \begin{pmatrix} f'(u_0) & -1 \\ 1/\tau & -1/\tau \end{pmatrix},$$

and

$$\mathbf{B} = \begin{pmatrix} f'(u_0) - D_u k^2 & -1 \\ 1/\tau & -D_v k^2/\tau - 1/\tau \end{pmatrix}.$$

Suppose that the system (6.12) is local stable, i.e.,

$$\begin{aligned} \mathrm{Sp}(\mathbf{A}) &= f'(u_0) - \frac{1}{\tau} < 0, \\ \mathrm{Det}(\mathbf{A}) &= -\frac{f'(u_0)}{\tau} + \frac{1}{\tau} > 0. \end{aligned}$$

Then we have

$$\begin{aligned} \mathrm{Sp}(\mathbf{B}) &= -\left(D_u + \frac{D_v}{\tau}\right) k^2 + \mathrm{Sp}(\mathbf{A}) \triangleq H(k), \\ \mathrm{Det}(\mathbf{B}) &= \frac{D_u D_v}{\tau} k^4 + \left(\frac{D_u - f'(u_0) D_v}{\tau}\right) k^2 + \mathrm{Det}(\mathbf{A}) \triangleq T(k). \end{aligned}$$

The critical wavenumber is

$$T'(k_c) = 0 \quad \Leftrightarrow \quad k_c = \sqrt{\frac{1}{2}\left(\frac{f'(u_0)}{D_u} - \frac{1}{D_v}\right)}$$

The instability occurs, if

$$T(k_c) \le 0 \quad \Leftrightarrow \quad f'(u_0) \ge 2\sqrt{\frac{D_u}{D_v}} - \frac{D_u}{D_v}.$$

Hence, the conditions (6.11) for the system (6.12) takes the form

$$\begin{aligned} &f'(u_0) < 1/\tau, \\ &f'(u_0) < 1, \\ &f'(u_0) > D_u/D_v, \\ &f'(u_0) \ge 2\sqrt{\frac{D_u}{D_v}} - \frac{D_u}{D_v}. \end{aligned} \tag{6.14}$$

Solving the system (6.14) with respect to $f'(u_0)$ we get

$$\begin{aligned} f'(u_0) &\in \left[2\sqrt{\frac{D_u}{D_v}} - \frac{D_u}{D_v}, \quad 1\right) \quad \text{if} \quad \tau < 1 \quad \text{and} \quad \frac{D_u}{D_v} < 1, \\ f'(u_0) &\in \left[2\sqrt{\frac{D_u}{D_v}} - \frac{D_u}{D_v}, \quad \frac{1}{\tau}\right) \quad \text{if} \quad \tau \geq 1 \quad \text{and} \quad \frac{D_u}{D_v} < 1/\tau. \end{aligned} \tag{6.15}$$

Let us discuss now the question, whether the Turing instability can occur by the change of some control parameter, e.g., κ_1. Indeed, from the fourth condition (6.14) can be seen that instability takes a place if $f'(u_0)$ at least equals to $2\sqrt{\frac{D_u}{D_v}} - \frac{D_u}{D_v}$, i.e.,

$$f'(u_0) = \lambda - 3u_0^2 = 2\sqrt{\frac{D_u}{D_v}} - \frac{D_u}{D_v} \triangleq \sigma,$$

whence it follows that

$$u_0 = \pm\sqrt{\frac{\lambda - \sigma}{3}}.$$

From the other hand u_0 is the homogeneous solution, so it satisfies

$$(\lambda - 1)u_0 - u_0^3 + \kappa_1 = 0$$

Hence, solving last two equations together we get the expression for the critical value κ_{1c} of the control parameter:

$$\kappa_{1c} = \pm\sqrt{\frac{\lambda - \sigma}{3}}\left(1 - \frac{2\lambda + \sigma}{3}\right). \tag{6.16}$$

Remark: Apart from varying some control parameter, a destabilization can be caused by increasing the system length. Indeed, if we assume to have a domain Ω of finite size with no-flux boundary conditions, the condition $k_l = \frac{l\pi}{\|\Omega\|}, l \in \mathbb{N}$ for possible modes in the system must be fulfilled [Purwins et al., 2005].

6.3 Turing instability in two-component RD system with an integral term

6.3.1 Influence of an integral term

In this section the influence of a global feedback, like, e.g., an integral term, on the conditions of Turing instability and pattern selection is discussed. For this purpose, consider a two-component reaction-diffusion system with an integral term, i.e.,

$$\begin{aligned} \partial_t u &= D_u \Delta u + f(u) - v + \kappa_1 - \kappa_2 \langle u \rangle, \\ \tau \partial_t v &= D_v \Delta v + u - v, \end{aligned} \tag{6.17}$$

where $\langle u \rangle$ denotes spatial average, describing the global feedback effect, namely

$$\langle u \rangle = \frac{1}{|\Omega|} \int_{\Omega} u(r,t) dr. \tag{6.18}$$

The homogeneous solutions (u_0, v_0) can be defined from the following system:

$$\begin{aligned} (\lambda - \kappa_2 - 1)u_0 - u_0^3 + \kappa_1 = 0, \\ v_0 = u_0. \end{aligned} \tag{6.19}$$

Similar to the previous sections we suppose that the homogeneous solution is stable in absence of diffusion and consider perturbations proportional to e^{ikr}. Since the mean value $\langle u \rangle$ is not equal to zero only for $k = 0$ the integral term can be replaced by the Kronecker symbol δ_{0k} and the matrix $\mathbf{B}$ may be written as:

$$\mathbf{B} = \begin{pmatrix} f'(u_0) - D_u k^2 - \kappa_2 \delta_{0k} & -1 \\ 1/\tau & -D_v k^2/\tau - 1/\tau \end{pmatrix}.$$

What this means is that presence of the integral term does not change the conditions of Turing instability (6.15). If we again choose κ_1 as a control parameter, the condition (6.16) for the system (6.17) takes a form:

$$\kappa_{1c} = \pm \sqrt{\frac{\lambda - \sigma}{3}} \left(1 + \kappa_2 - \frac{2\lambda + \sigma}{3} \right). \tag{6.20}$$

The value σ has here the same meaning as in the previous section.

6.3.2 Numerical results

As has been shown above the presence of the integral term does not disturb the conditions of Turing instability, only homogeneous steady state and corresponding critical values of control parameter are shifted on κ_2. At the first glance it seems as if the integral term does not play any role in formation of spatial periodic structures. A detailed discussion of this problem in one spatial dimension in the terms of amplitude equation was treated in [Dohmen, 1991, Or-Guil, 1997]. In particular, it was shown, that parameter λ plays an important role, namely, its change can cause the transition of the homogeneous system to *super-* and further to *subcritical* regime. In this context, a supercritical bifurcation means the transition from homogeneous stable state to spatial periodic pattern, which amplitude increases continuously beyond the threshold. In this case, the integral term can affect only the amplitude of the resulting periodical pattern, but not the pattern itself. In contrast, in subcritical regime the presence of integral term has an influence, namely, of above the threshold the amplitude the spatial pattern jump up to some constant value. Moreover, resulting pattern is not periodic in space, but only some wave trains emerge. By further change of the control parameter, (e.g, κ_1) the number of

periodical domains increases until the whole domain is periodic in space. Further increase or decrease of κ_1 leads again to appearance of the separated periodic domains, which number decreases with the change of the control parameter until the whole domain becomes homogeneous (see Fig. 6.2). Notice, that a small hysteresis region (see Fig. 6.2 for $\kappa_1 = -1.75$) exists, indicating a subcritical "nature" of the transition.

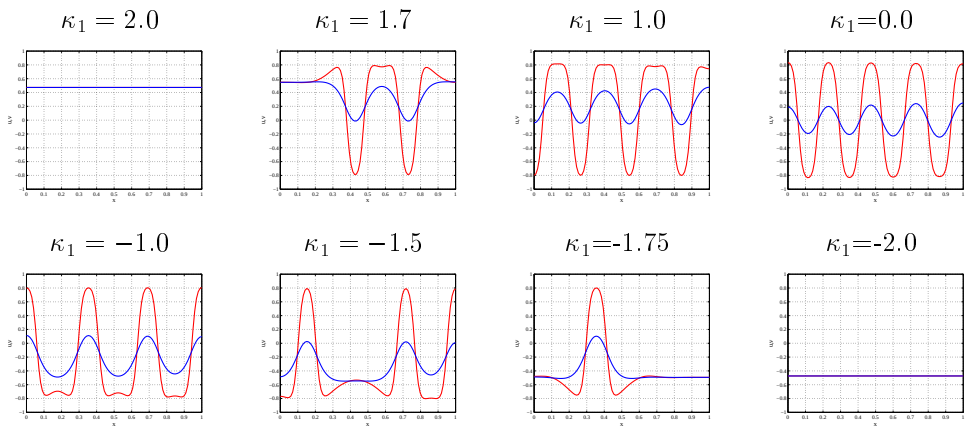

FIG. 6.2: Subcritical Turing instability in one-dimensional case. Behavior of activator (red) and inhibitor (blue) distributions for different control parameter values is shown. Parameters: $D_u = 2.8 \cdot 10^{-4}$, $D_v = 5 \cdot 10^{-3}$, $\lambda = 1.0$, $\kappa_3 = 1.0$, $\kappa_2 = 4.0$, $\tau = 1.0$; the critical value of the control parameter $\kappa_{1c} = \pm 1.708$. Computation was performed on the domain $\Omega = [0,\ 1]$ with no-flux boundary conditions.

Let us now discuss the subcritical Turing bifurcation in two-dimensional space. For this purpose we have solved the system (6.17) numerically at different values of the control parameter κ_1 with zero-flux boundary conditions on a rectangular domain $\Omega = [0, 5] \times [0, 5]$. In the beginning, for the given parameter set, the value of κ_1 is set to the value, corresponding to the stable homogeneous solution and the initial condition is chosen to be the random perturbed homogeneous solution. When the simulation reaches a stationary state, a further simulation is started with decreased κ_1 and with the previous stationary state as the initial condition. In this way, we can calculate the emerging patterns for all $\kappa_1 \in [-\kappa_{1c}, \kappa_{1c}]$, where $\pm\kappa_{1c}$ are defined by Eq. (6.20). Notice that one can consider two different simulation series, one for decreasing and one for increasing κ_1. In Figs. 6.3,6.4 an example from these series are to be seen. Figure 6.3 shows the resulting patterns for increased values of κ_1. For $\kappa_1 < -\kappa_{1c}$ the system (6.17) has homogeneous stable state $(u_0, v_0)^T$. Above the threshold $-\kappa_{1c}$ the uniform state becomes unstable in favor of finite wave number perturbation. That is, starting with random perturb homogeneous solution one obtains a high-amplitude spot-like pattern, shown in Fig. 6.3 for $\kappa_1 = -1.65$. Notice, that as the system is in a subcritical regime (forcing a high-amplitude pattern) and because of the presence of the integral term (lim-

iting the overall activator density), the pattern is not periodic in space, but only some wave trains emerge. This pattern is stable on a quite long timescale with a slow tendency to agglomerate the bright spots. In the course of further decrease of κ_1 the pattern significantly changes its shape:spot-like pattern (see, e.g., Fig. 6.3 for $\kappa_1 = -1.0$ and $\kappa_1 = -0.5$), stripes (or labyrinths) ($\kappa_1 = 0.5$), labyrinth patterns with holes for relatively high parameter values ($\kappa_1 = 1.0$ and $\kappa_1 = 1.5$). Finally, one observes spot-like patterns with low u (dark) spots on a high u (bright) background ($\kappa_1 = 2.0$, $\kappa_1 = 2.5$, $\kappa_1 = 2.6$). In contrast to the previously seen, Turing triggered patterns, these spots do not form coherent wave trains. The number of spots decreases for increasing values of κ_1. When κ_1 passes through 2.62, the pattern vanishes and the homogeneous solution emerges (see fig. 6.3, $\kappa_1 = 3.0$). This second critical value of κ_1, being different from κ_{1c}, we refer to as κ_{1h}.

The same patterns behavior with exchanged dark (low u) and bright (high u) areas can be observed for decreasing values of the control parameter κ_1 (see Fig. (6.4)). In this case the onset of the Turing instability then occurs at $\kappa_{1c} = 1.608$, and at $\kappa_{1h} = 2.72$ the pattern vanishes.

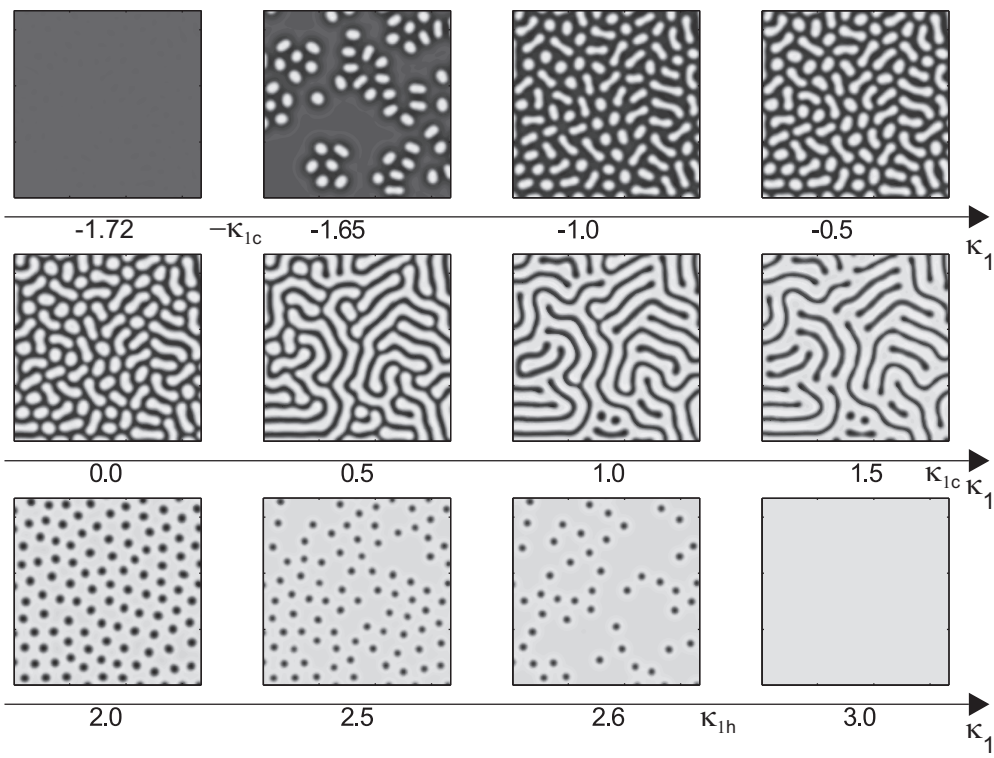

FIG. 6.3: Typical high-amplitude patterns corresponding to the nonuniform solutions of the system (6.17) if κ_1 is increased. Parameters: $D_u = 2.8 \cdot 10^{-4}$, $D_v = 5.0 \cdot 10^{-3}$, $\lambda = 0.9$, $\kappa_2 = 4.0$, $\tau = 1.0$, $\kappa_1 \in [-3.0, 3.0]$, $\Omega = [0,\ 5] \times [0,\ 5]$, boundary conditions are Neumann. The critical values $\kappa_{1c} = \pm 1.709$.

To investigate the type of the observed bifurcations, we calculate from the

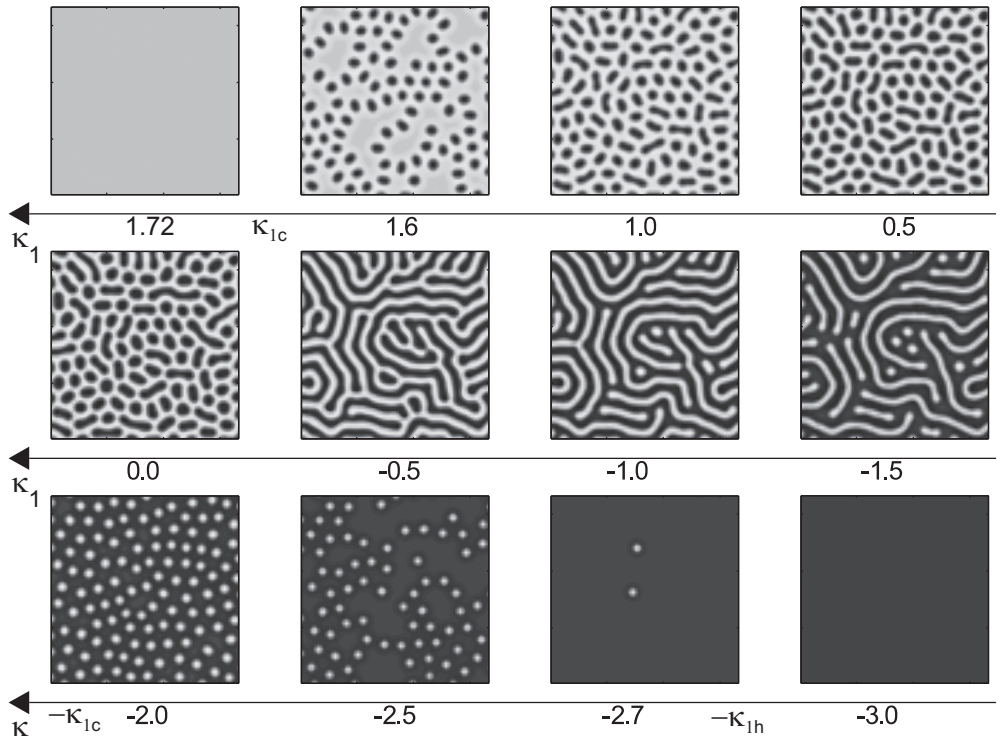

FIG. 6.4: Typical patterns arising in the system (6.17) if κ_1 is decreased. Parameters: $D_u = 2.8 \cdot 10^{-4}$, $D_v = 5.0 \cdot 10^{-3}$, $\lambda = 0.9$, $\kappa_2 = 4.0$, $\tau = 1.0$, $\kappa_1 \in [-3.0, 3.0]$, $\Omega = [0,\ 5] \times [0,\ 5]$, boundary conditions are Neumann. The critical values $\kappa_{1c} = \pm 1.709$.

results gained numerically the pattern amplitude difference A_{th} of the activator u as a function of κ_1. A_{th} is defined as the difference between the largest and the smallest value of u within Ω. Due to the used numerical accuracy a noise rejection for u is not necessary. The result is shown in fig. 6.5 for decreasing (solid triangles) and increasing (open triangles) κ_1.

On this background the behavior of the system can be understood as follows: for $|\kappa_1| > \kappa_{1h}$ the system (6.17) is in a homogeneous stable state, corresponding to the zero amplitude A_{th} . For $|\kappa_1| < \kappa_{1c}$ the system is in a patterned state. The amplitudes A_{th} for all parameter values in this region are almost the same. The bifurcations taking place if $|\kappa_1|$ crosses κ_{1c} or κ_{1h} are subcritical. For $|\kappa_1| \in [\kappa_{1c}, \kappa_{1h}]$ there are hysteresis regions, i.e. the actual value of the amplitude A_{th} is determined by the initial condition of the calculation, i.e. the direction of κ_1 variation. The patterns in these regions consist of solitary spots being not connected to each other (see fig. 6.3).

6.3.3 Experimental observations

Bifurcation scenario and patterns, described above are known from other RD models, describing, e.g., some chemical systems [Peña and Pérez-García, 2001] or vegetation processes [Meron et al., 2004]. Experimental observa-

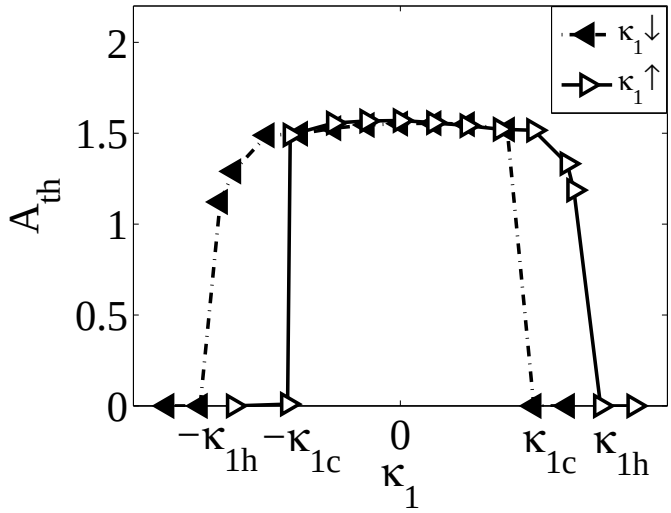

FIG. 6.5: Dependence of the amplitude on the control parameter for increased (△) and decreased (▲) values of κ_1. Parameters: $D_u = 2.8 \cdot 10^{-4}$, $D_v = 5.0 \cdot 10^{-3}$, $\lambda = 0.9$, $\kappa_2 = 4.0$, $\tau = 1.0$, $\kappa_1 \in [-3.0, 3.0]$. The critical values $\kappa_{1c} = \pm 1.608$.

tions of such solitary filaments and spatially periodic patterns in quasi-one-dimensional dc gas-discharge system ([Willebrand et al., 1990]) or p-n-p-n semiconductor structures ([Niedernostheide et al., 1992b]) have also been accomplished, but experimental observations in two-dimension are rare in occurrence [von Hardenberg et al., 2001]. Recently transition from bright to dark solitary filaments was found in dielectric barrier discharge system (DBD) with a large aspect ratio []. This system is know to produce a large amount of varying patterns, both particle-like structures [Dong et al., 2001, Müller et al., 1999, Stollenwerk et al., 2006, Brauer, 2000] and other spatial patterns [Gurevich et al., 2003b]. Usually, solitary filaments in such systems occur as current channels perpendicular to the dielectric barriers, defining a spot in the 2-dimensional discharge plane. These well localized objects and the corresponding well localized luminescence radiation density distribution we refer to as bright dissipative solitons. In the present experiments also dark solitons occur, consisting of a currentless, dark spot in an otherwise bright, homogeneous discharge. To obtain the transition between these two types of solitons only a single system parameter has to be varied. The intermediate states consist of different stripe-like patterns.

The experimental set-up is sketched in Fig. 6.6. Both electrodes consist of glass plates coated with Indium Tin Oxide (ITO), which is electroconductive and transparent with respect to the luminescence radiation being emitted from the gas during discharge. The latter being captured by appropriate cameras is to good approximation proportional to the current density. Between the glass plates there is a dielectric spacer defining a circular discharge area with diameter $D = 40$ mm and thickness $d = 0.5$ mm being the discharge length. One of